AIP | The Journal of Chemical Physics

An experimental and mechanistic study of the reactions of COF2 with H2 and with CO

H. J. Gangloff, D. Milks, K. L. Maloney, T. N. Adams, and R. A. Matula

Citation: The Journal of Chemical Physics **63**, 4915 (1975); doi: 10.1063/1.431235
View online: http://dx.doi.org/10.1063/1.431235
View Table of Contents: http://scitation.aip.org/content/aip/journal/jcp/63/11?ver=pdfcov
Published by the AIP Publishing

An experimental and mechanistic study of the reactions of COF_2 with H_2 and with CO

H. J. Gangloff, D. Milks, K. L. Maloney*, T. N. Adams†, and R. A. Matula

Combustion Kinetics Laboratory, Mechanical Engineering and Mechanics Department, Drexel University, Philadelphia, Pennsylvania 19104

(Received 2 January 1973)

The decomposition of carbonyl fluoride (COF_2), the reactions of carbonyl fluoride with carbon monoxide (CO), and the reactions of carbonyl fluoride with hydrogen (H_2) in excess argon were studied behind reflected shock waves. Kinetic data were obtained in the temperature and total pressure ranges 2600–3300 °K and 2.5–9.0 atm, respectively, for the COF_2 decompostion study, in the temperature and total pressure ranges 2400–3000 °K and 3.3–7.7 atm, respectively, for the COF_2–CO study, and in the temperature and total pressure ranges 1900–2700 °K and 2–12 atm, respectively, for the COF_2–H_2 study. Under the experimental conditions, the bimolecular reaction between COF_2 and CO was found to be negligible with respect to the decomposition of COF_2. An empirical relationship for the over-all kinetics of the COF_2–H_2 reaction was determined, and a combined analytical and experimental study was conducted to determine a plausible mechanism for the COF_2–H_2 reaction. Under the experimental conditions, the dominant reaction steps in this mechanism were determined to be $COF_2+M \rightarrow_{k_1} COF+F+M$, $COF+M \rightarrow_{k_2} CO+F+M$, $H_2+M \rightarrow H+H+M$, $F+H_2 \rightarrow HF+H$, $H+COF_2 \rightarrow_{18} COF+HF$, $H+COF \rightarrow_{20} CO+HF$. In these studies an experimental value of k_1 was obtained as $k_1 = 10^{14.25\pm0.24}\exp(-77\,200 \pm 3300/RT)$ cc/mole·sec. The rate constant for Reaction 2 was derived based on experimental data, a steady state analysis, and an estimate of the ratio of the rate constants of Reactions 18 and 20. The derived value for k_2 is given as $k_2 = 10^{15.0}\exp(-49\,000/RT)$ cc/mole·sec. The heat of formation of COF at absolute zero was determined to be approximately equal to −66 kcal/mole relative to the JANAF standard state definition.

I. INTRODUCTION

Currently there is interest in the combustion of fluorocarbons, in which carbonyl fluoride (COF_2) has been found to be an important product. Therefore, the development of a mechanism for the production and subsequent reaction of COF_2 with compounds which frequently occur in high temperature fluorocarbon combustion systems is of importance. The high temperature thermal decomposition of COF_2 has been shown to be unimolecular in the temperature range 2200–3600 °K.[1,2] Modica[1] reported the pressure and temperature dependence of the experimentally determined rate constant for the decomposition of COF_2 in terms of Rice–Ramsperger–Kassel (RRK) unimolecular theory, and Weston and Matula[2] analyzed the variation of the observed rate constant with pressure and temperature in terms of both the RRK and the Lindemann theories and reported that the Lindemann theory better fitted the experimental data. The numerical values of the COF_2 decomposition rate constants reported by the two groups of researchers were in general agreement, but the numerical value of the high pressure limiting rate constant for COF_2 decomposition reported in Ref. 2 was approximately one-sixth of that reported in Ref. 1.

The mechanism in Table I for the thermal decomposition of COF_2 in the temperature range of 2200–3600 °K and at total pressures between 0.2–26 atm has been postulated in Ref. 1. It was reported[1] that, in certain instances, the elementary reaction step $COF_2 + CO \rightarrow COF + COF$ dominates the unimolecular decomposition of COF_2 after approximately 20% of reaction. The implication of this is that the addition of CO to a system with COF_2 would enhance the disappearance rate of COF_2. In light of this, the present experimental program was undertaken to study the bimolecular reaction between COF_2 and CO. The addition of H_2 to a COF_2–Ar mixture was found to increase significantly the reaction rate of COF_2. Since the COF_2–H_2 reaction system has not been previously studied, a program was conducted to investigate in detail the reaction of COF_2 with H_2 and to ascertain the mechanism by which the reaction rate of COF_2 is enhanced.

II. EXPERIMENTAL METHODS

The shock tube facility employed in this study has been described in detail previously.[2,3] The initial temperatures and concentrations behind the reflected shock waves were calculated by an in-house computer program

TABLE I. Mechanism and rate constants for COF_2 decomposition proposed by Ref. 1.

Reaction	Rate constant
$COF_2 \xrightarrow[Ar]{1^1} COF + F$	$8.52\times10^{8}\, e^{-46\,257/T}\int_0^\infty \frac{x^6 e^{-x}\,dx}{1+\frac{8.19\,T^{-0.5}}{[M]}\left[\frac{x}{(46\,257/T)+x}\right]^6}$
$COF \xrightarrow{2} CO + F$	$1.02\times10^{11}\, e^{-34\,510/T}\int_0^\infty \frac{x^3 e^{-x}\,dx}{1+\frac{2.05\,T^{-0.5}}{[M]}\left[\frac{x}{(34\,510/T)+x}\right]^3}$
$COF_2 + F \xrightarrow{3} COF + F_2$	$1.0\times10^{12}\, T^{0.5}\, e^{-27\,740/T}$
$COF + F_2 \xrightarrow{4} COF_2 + F$	$4.72\times10^{10}\, T^{0.5}\, e^{1037/T}$
$COF + F \xrightarrow{5} CO + F_2$	$1.0\times10^{13}\, T^{0.5}\, e^{-16\,429/T}$
$COF + COF \xrightarrow{6} COF_2 + CO$	$1.07\times10^{9}\, T^{0.5}\, e^{695/T}$
$COF_2 + CO \xrightarrow{7} COF + COF$	$1.0\times10^{11}\, T^{0.5}\, e^{-11\,656/T}$
$F_2 + Ar \xrightarrow{8} F + F + Ar$	$1.52\times10^{12}\, e^{-12\,038/T}$
$F + F + Ar \xrightarrow{9} F_2 + Ar$	$1.46\times10^{11}\, e^{6097/T}$

[M] = total concentration

Units of cubic centimeters, °K, mole, sec

In paper superscript 1 denotes a first order rate constant and reaction.

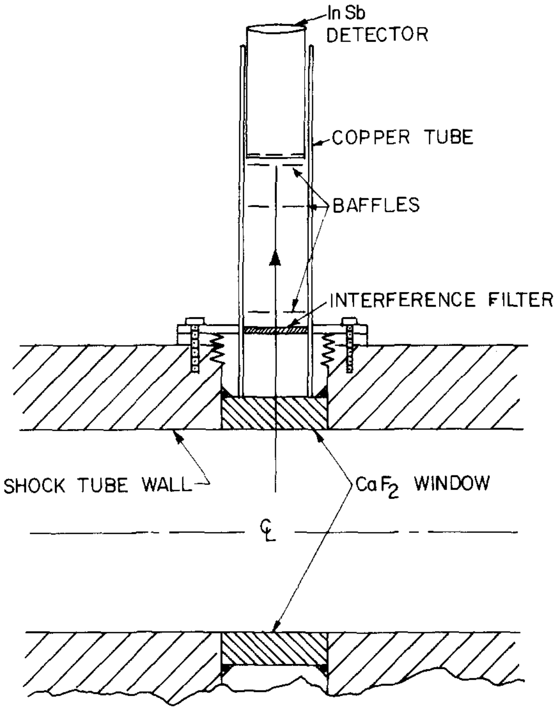

FIG. 1. Schematic diagram of shock tube infrared spectroscopic system.

according to the standard conservation equations as a function of the measured incident shock velocity assuming no reaction behind either the incident or reflected wave. The enthalpy data required for the computations were obtained from the JANAF[4] tables and fitted to fourth order polynomials in temperature. The optical arrangement described in Ref. 2 was replaced by that in Fig. 1. This was done in order to achieve a better signal to noise ratio and to improve the response time of the optical system. A Perry model 720 preamplifier, modified to operate linearly with a reactive source, was employed to extend the bandwidth of the amplifier system to greater than 500 kHz. The output of this amplifier was used to drive a Tektronix 3A9 vertical amplifier in a Tektronix 565 oscilloscope. Electronic response time with these components was limited to approximately 1 μsec by the InSb detector.

In these studies, the 5.15 μ fundamental band of COF_2 and the 2.51 μ fundamental band of HF were monitored with a Philco type ICS 391C Indium Antimonide detector. The radiation emitted by the COF_2 was filtered by a 5.18 μ long pass filter, which when used with the InSb detector gave the relative optical response previously described in Ref. 2. The HF radiation was filtered using a 2.51 μ narrow pass filter. In the present work, the overlap of the 4.66 μ band of CO, which is produced from the decomposition of COF_2 and is added in the COF_2–CO system, resulted in a slight increase in the radiation indicated on the emission oscilloscope traces. For the COF_2–CO system this radiation increase was approximately 5%–10% of the total radiation seen by the experimental system over the experimental conditions. This effect is shown in Fig. 2, where the increase in radiation with 1% added CO to the 1% COF_2–Ar system is 8% over the pure 1% COF_2–Ar system at the same temperature and total concentration. In all cases, this overlap of the CO radiation whether from CO resulting from the decomposition of COF_2 or added CO had a negligible effect on the calculated rate constants when compared to the over-all experimental uncertainty. No spectral overlap from other emitting species was observed in the HF experiments.

In all the studies, the initial concentration of COF_2, being a reactant, was assigned the value predicted by the shock tube program, and the experimental detector signal was measured immediately behind the reflected shock waves. To determine the effect of optical depth on the measurement of the COF_2 concentration as a function of detector signal, plots of detector signal vs COF_2 concentration were obtained from experimental data for various isotherms. In addition, a relative theoretical signal was calculated as a function of COF_2 concentration by the following integral,

$$S_r = \int_{\nu_1}^{\nu_2} (1 - \exp[-P_\nu(T) n l]) I_\nu(T) R_\nu \, d\nu ,$$

where n is the concentration of COF_2 in moles/cc; l is

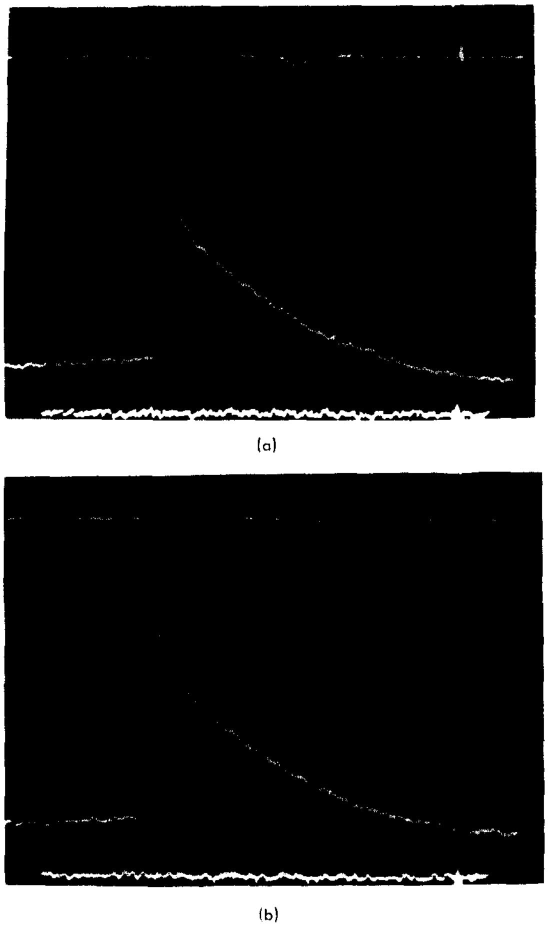

FIG. 2. Comparison oscilloscope traces of the COF_2 and COF_2–CO studies: (a) 1% COF_2 in argon, $T = 2985\,°K$; $[M] = 0.21 \times 10^{-4}$ moles/cc; (b) 1% COF_2, 1% CO in argon, $T = 3025\,°K$; $[M] = 0.2135 \times 10^{-4}$ moles/cc. Centered in each photograph is the emission trace of COF_2. Vertical axis is COF_2 emission voltage and horizontal axis is reaction time. Upper trace indicates arrival of shock wave seen by piezoelectric transducer.

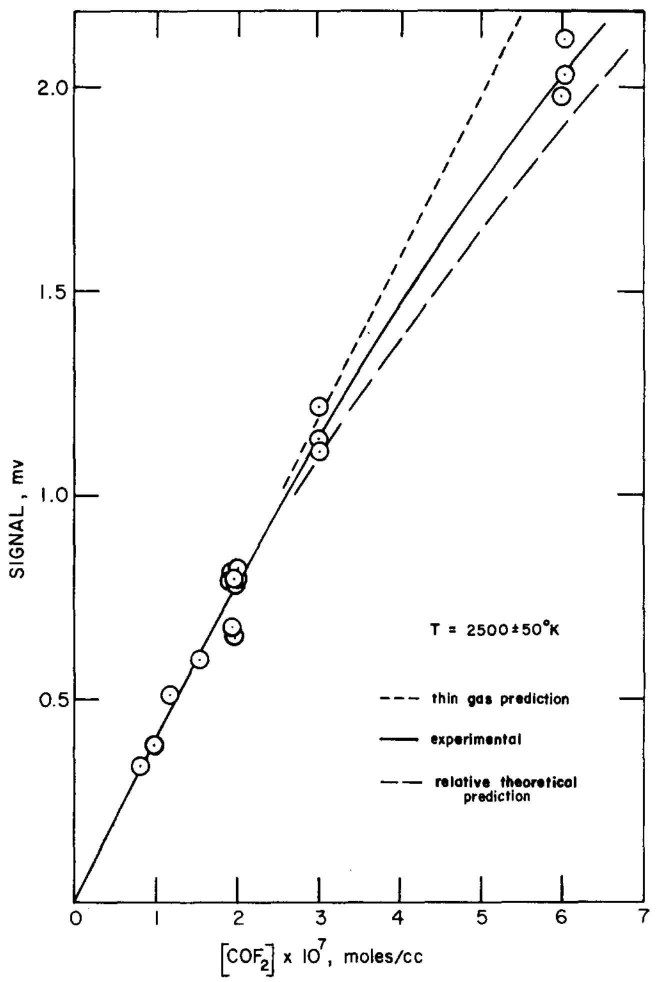

FIG. 3. Comparison of the experimental and theoretical optical depth results.

the tube diameter, in centimeters; ν_1, ν_2 are the lower and upper bounds of the systems optical response, in cm^{-1}; $P_\nu(T)$ is the spectral intensity, in cm^{-1} $(mole/cc)^{-1}$; $I_\nu(T)$ is the blackbody radiancy, in $watts/cm^2/cm^{-1}/$ steradian; and R_ν is the relative optical response of the filter and detector. The spectral intensity, $P_\nu(T)$, was calculated by the methods of Adams, *et al.*[5] and fitted as a function of ν for various temperatures. The relative optical response of the system, R_ν, was also fitted as a function of ν. The analysis for a temperature of 2500 ± 50 °K is shown in Fig. 3 with a least squares fit of the experimental data plotted vs COF_2 concentrations. The integrated relative theoretical prediction, plotted in Fig. 3, was matched with the experimental data at low COF_2 concentrations. The detector signal is approximately directly proportional to the COF_2 concentration below concentrations of 4×10^{-7} mole/cc, and both the experimental data and the theoretical calculation show a deviation from the thin gas prediction above 4×10^{-7} mole/cc. Only three experimental rate data points were obtained which had COF_2 concentrations in excess of the limiting concentrations, and these were corrected to take into account optical depth.

In the COF_2–H_2 study, the time dependent concentration of HF, being a reaction product, was determined by first examining the detector signal of the equilibrium concentration of HF as indicated on the HF emission oscillograms. The equilibrium concentration of HF was determined by assuming that all of the hydrogen is reacted to HF when the stoichiometry indicated that there is more available fluorine than hydrogen, or that all of the fluorine is reacted to HF when the available hydrogen is greater than fluorine. This technique was based on equilibrium calculation of the COF_2–H_2 system. To verify this assumption, a 2% mixture of HF was shock heated and the emission level was compared to the equilibrium emission level of HF for a shock reacted 1% H_2, 1% COF_2 mixture. In line with the above assumption, the equilibrium concentration of HF would be twice the initial concentration of H_2 for the 1% H_2, 1% COF_2 mixture. The results of these experiments indicated that this assumption was valid in that the HF emission levels for the 2% HF mixture were in good agreement with the equilibrium levels of HF for the 1% H_2, 1% COF_2 mixture. No corrections due to temperature change during the reaction were incorporated in assigning the HF concentration since computer simulation of the reaction mechanism, and the energetics of the over-all reaction of $COF_2 + H_2 \rightarrow 2HF + CO$ showed little temperature change. Based on the equilibrium values of the HF concentration, the emission signal of HF was found to be proportional to the concentration of HF and independent of temperature in the temperature and total concentration ranges, 2000–2500 °K and 1.8–3.8×10^{-5} mole/cc, respectively.

For comparison with the experimental COF_2 and HF concentration profiles, two computer programs were used to compute concentration and temperature variation of the test gases as a function of reaction time for the kinetic mechanisms. Computations were carried out assuming that the reactions behind the reflected shock wave proceeded adiabatically and at a constant volume. Some of the computations were carried out on a CDC 6600 computer employing a kinetics program developed by Ref. 6. An in-house computer program, which was written for a Wang Model 700B advanced programmable calculator, was also developed for each of the systems of interest. The results of the two programs were checked for a number of typical cases in order to assess the validity of the in-house computations, and in all cases, both the temperature and concentration profiles generated by the two techniques agreed to within 0.5 to 1.0%. Since the in-house program was more economical, most of the numerical computations were carried out on the Wang computer. Corrections due to boundary layer effects were not included in the computations in light of previous arguments.[3]

The COF_2 used in these studies was purchased from Peninsular Chem Research, Gainesville, FL. The supplier specified that the purity of the COF_2 was 99%. However, subsequent mass spectroscopic, gas chromatographic, and infrared analysis of the COF_2 in our laboratory showed that the COF_2 had a 3% CO_2 impurity and a trace of CF_4. Chemically pure grade carbon monoxide (minimum purity 99.5%), ultrapure hydrogen (minimum purity 99.999%), and ultrapure argon (minimum purity 99.995%) were all purchased from Matheson

TABLE II. Molar composition of test mixtures utilized in conjunction with the COF_2, COF_2–CO, and COF_2–H_2 reaction studies.

Mixture	COF_2	H_2	CO
1	1%		
2	1/2%	1%	
3	1%	1%	
4	1%	2%	
5	1%	4%	
6	1%		1%
Balance is argon			

Co. The helium (minimum purity 99.999%) and hydrogen fluoride (minimum purity 95%) were purchased from Air Products. During the course of the experiments, helium was used as a driver gas and argon was employed as a diluent gas. All gases were used as received from the suppliers.

The molar compositions of the six test mixtures used during the course of these studies are listed in Table II. The test mixtures were prepared utilizing standard manometric techniques and stored in passivated stainless steel tanks. All test mixtures were allowed to mix thoroughly prior to use. The precautions in handling COF_2, in particular, the necessity of precluding water from the system,[2] were adhered to in the present studies.

III. EXPERIMENTAL RESULTS

A. COF_2 decomposition studies

Since a knowledge of the unimolecular decomposition rate of COF_2 in the absence of CO and H_2 was of importance to this study, a brief reinvestigation of the thermal decomposition of COF_2 was carried out in the temperature and total pressure ranges 2600–3300 °K and 2.5–9.0 atm, respectively. The study was conducted using techniques similar to those described in Refs. 1 and 2 so that the results of this study could be compared to those of the previous studies. The initial slopes of the COF_2 infrared emission oscillograms were used to compute the experimental rate constant values. The numerical value of the observed first order rate constant, k_1^1, for

$$COF_2 \xrightarrow{k_1^1} COF + F$$

reported by Ref. 2 as a Lindemann fit is approximately a factor of 2 lower than the values obtained in the present study, while the RRK expression of Ref. 1 yields first order values of k_1^1 that are 3–4 larger than the present results (see Table III).

The data obtained in the present study on the decomposition of COF_2 were also fitted to a second order expression with excellent results. The experimental first order values of k_1^1 ($\sec^{-1}$), listed in Table III, were expressed as second order rate constants, k_1 (cc/mole · sec), and are shown graphically in the Arrhenius plot of Fig. 4. The best fit to these data resulted in a rate constant for $COF_2 + M \xrightarrow{k_1} COF + F + M$ of

$$k_1 = 10^{14.25\pm0.24} \exp\left(\frac{-77\,200 \pm 3300}{RT}\right) \text{ cc/mole} \cdot \text{sec} . \qquad (1)$$

Total concentrations in the present COF_2 decomposition study were lower than in the previous studies reported in Refs. 1 and 2. This may account for the fact that the previous investigators correlated their rate data in terms of various unimolecular expressions. The second order rate constant for $COF_2 + M \xrightarrow{k_1} COF + F + M$ given by Eq. (1) from this study will be employed throughout the remainder of this paper.

B. Bimolecular reaction between CO and COF_2

Based on the postulated mechanism[1] in Table I, the initial rate of COF_2 disappearance in a 1% CO, 1% COF_2 mixture in argon at 2700 °K should increase by a factor of 7.9 over the COF_2 disappearance rate in a pure 1% COF_2 in argon mixture when the value of k_7 given in Table I is used in conjunction with the value for k_1 given by Eq. (1). In order to study the effect of adding CO to a COF_2 mixture, a 1% CO, 1% COF_2, and 98% Ar mixture was prepared, and the initial rate of COF_2 decomposition in the temperature and pressure ranges 2400–3000 °K and 3.3–7.7 atm was studied. The initial observed rate of decomposition of COF_2 was measured from the initial slope of the infrared emission oscillo-

TABLE III. Comparison of the literature values of the first order rate constant, k_1^1($\sec^{-1}$), for $COF_2 \xrightarrow{k_1^1} COF + F$ with the results obtained in this study.

$10^4/T$	$[M]\times10^5$	k_{obs}^1	k_{obs}^1/k_{WM}^1	k_{Modica}^1/k_{obs}^1
3.4	1.05	3077	1.5	5.5
3.05	1.30	18670	2.8	4.0
3.0	2.17	33330	2.7	3.7
3.05	1.73	18920	2.2	4.7
3.73	3.20	2414	1.5	3.1
3.54	3.91	5000	1.7	3.1
3.48	2.90	5833	1.6	3.5
3.42	2.91	7368	1.7	3.5
3.52	2.90	7568	1.7	3.4
3.81	2.80	2546	2.2	2.0
3.29	2.10	11920	2.3	3.1
3.33	2.08	8750	1.9	3.65
3.35	2.08	8750	2.1	3.3
3.31	2.09	8750	1.8	4.0
3.43	2.09	7778	2.3	2.7
3.41	2.09	6667	1.9	3.5
3.35	2.10	8750	2.1	3.3
3.48	2.08	3810	1.3	4.6
3.14	2.14	18420	2.25	3.9
3.59	2.06	3294	1.65	3.3
3.61	2.05	3011	1.6	3.3
3.69	2.02	2154	1.5	3.3
3.22	1.27	8974	2.2	4.25
3.0	2.17	33330	2.7	3.7
3.32	1.26	7778	2.5	3.3

Units of cubic centimeters, °K, mole, sec.; [M] = total concentration.

k_{obs}^1: this study k_1^1, where $k_{obs}^1 \equiv \left.\frac{-1}{[COF_2]_0}\frac{d[COF_2]}{dt}\right|_0$

k_{Modica}^1: see Table I for k_1^1 of Ref. 1 (RRK fit)

k_{WM}^1: Ref. 2 k_1^1 (Lindemann fit)

$$\frac{1}{k_{WM}^1} = \frac{1}{1.28\times10^{11}\exp(-93\,300/RT)} + \frac{1}{1.15\times10^{12}\exp(-49\,700/RT)[M]}$$

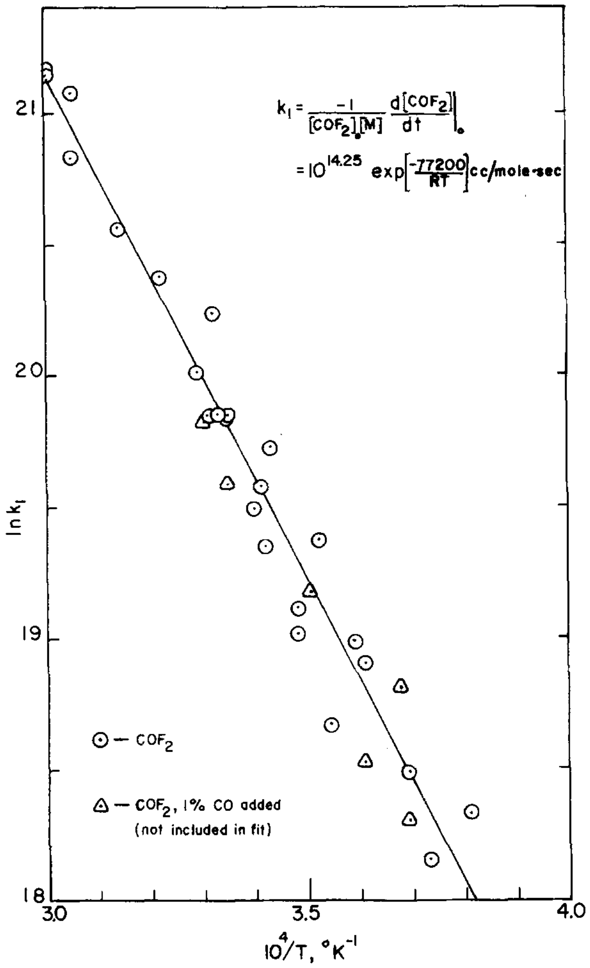

FIG. 4. Arrhenius plot of the low pressure unimolecular decomposition of COF_2.

grams, and this result was utilized to compute a numerical value of the first order $k^1_{obs\text{-}CO}$ defined by

$$k^1_{obs\text{-}CO} \equiv -\frac{1}{[COF_2]_0} \left.\frac{d[COF_2]}{dt}\right|_0 \qquad (2)$$

where the subscript 0 denotes initial conditions. The observed first order rate constants for data obtained in the COF_2–CO study are listed in Table IV along with the numerical value of $k_1[M]$ for comparison where k_1 is given by Eq. (1). The COF_2–CO data are also plotted in Arrhenius form in Fig. 4 as second order rate constant values for comparison with the second order k_1 given by Eq. (1).

Inspection of the results in Table IV and Fig. 4 indicates that the observed rate constant for the initial rate of decomposition of COF_2 is not measurably enhanced by the addition of 1% CO to the 1% COF_2 mixture. If these rate data were corrected for the 5%–10% overlap emission of the CO 4.66 μ band, the agreement between the COF_2–CO and pure COF_2 data in both Table IV and Fig. 4 would be even better. However, a 5%–10% correction of the rate data is not justified, considering the experimental scatter in Fig. 4. Based on these results, it is suggested that the value of the estimated rate constant k_7, for the bimolecular reaction between CO and COF_2, listed in Table I from Ref. 1 is at least a factor of 15 higher than is justified by the present experiment. This COF_2–CO system experimental result was used subsequently to estimate the rate constants and the effects of Reaction (7) and its reverse reaction, Reaction (6), on both the pure COF_2 study and the COF_2–H_2 study. For the experimental conditions, the computer integrated simulations of the studies indicated that these COF_2–CO reactions were insignificant (see Sec. V).

C. Reaction of COF_2 in the presence of hydrogen

The kinetics of the COF_2–H_2 reaction system was studied in the temperature and total pressure ranges 1900–2700 °K and 2–12 atm, respectively, behind reflected shock waves. The variation of COF_2 concentration with time was obtained from infrared emission oscillograms, and in some of the experiments the rate of formation of HF was monitored with the aid of infrared emission spectroscopy. The observed initial reaction rates of COF_2 and HF were obtained from the initial slope of the appropriate emission traces. The initial rate data were taken over the first 30%–40% of COF_2 reaction and HF production since the infrared emission records displayed a high degree of linearity in this region. No corrections to the rate data were made due to temperature change during the reaction since it was shown that the computed temperature changes during typical reaction times were on the order of 1%.

A series of experiments was carried out using the four H_2–COF_2–Ar mixtures listed in Table II in order to evaluate an empirical rate expression that could be employed to predict the initial rate of COF_2 decompostion in the presence of H_2 in the temperature range 1900–2700 °K. An empirical rate expression of the form

$$\left.\frac{d[COF_2]}{dt}\right|_0 = -k_{obs\text{-}H_2}[COF_2]_0^a[H_2]_0^b[M]^c \qquad (3)$$

was tested, and a least mean squares fit of the data resulted in an expression of the form

TABLE IV. Comparison of the observed rate constants for the initial rate of decomposition of COF_2 with and without added CO.

$10^4/T$	$[M]\times10^5$	$k^1_{obs\text{-}CO}$	$k_1[M]$
4.117	3.975	614	799
3.360	2.115	6829	8 039
3.306	2.135	8750	10 030
3.508	2.112	4516	4529
3.679	2.079	3111	2288
3.691	2.078	1854	2181
3.622	2.084	2333	2866

[M] = total concentration

Units of cubic centimeters, °K, mole, sec

$k^1_{obs\text{-}CO} \equiv \frac{-1}{[COF_2]_0} \left.\frac{d[COF_2]}{dt}\right|_0$ (study with added CO)

$k_1\,[M] = \frac{-1}{[COF_2]_0} \left.\frac{d[COF_2]}{dt}\right|_0$ (study without added CO)

$k_1 = 10^{14.25}\exp(-77\,200/RT)$ cc/mole · sec

TABLE V. Varaition of the empirical rate constant for the reaction of COF_2 in the presence of H_2.

Mixture	$10^4/T$	$[M]\times 10^5$	$k_{obs\text{-}H_2}\times 10^{-7}$
2	4.165	1.909	24.04
2	4.080	1.920	33.15
2	3.632	1.998	133.5
2	3.8655	1.957	60.88
2	3.761	1.979	101.1
2	3.902	1.952	56.25
2	4.564	1.862	7.941
2	4.415	1.887	11.51
2	4.871	1.812	2.671
2	4.975	1.794	2.168
2	4.744	1.831	4.484
2	3.843	3.955	64.36
2	4.401	3.761	13.79
2	4.780	3.636	3.182
2	4.034	3.887	36.02
3	4.753	5.649	2.986[a]
3	3.885	0.9213	126.7
3	4.3085	3.865	24.55
3	4.296	2.902	20.53
3	4.2845	1.938	24.90
3	4.186	1.954	45.51
3	4.246	2.912	24.65
3	4.419	2.866	12.69
3	4.346	2.884	17.65
3	4.077	1.971	49.01
3	4.003	1.980	70.71
3	4.787	3.678	3.458
3	4.543	3.757	6.902
3	4.382	3.814	12.04
3	4.196	3.874	34.43
3	4.124	2.927	44.47
3	4.307	2.872	22.42
3	3.994	2.001	69.96
3	4.261	1.943	24.09
3	4.054	1.989	54.16
3	4.496	1.911	10.54
3	4.1135	1.981	41.59
3	3.934	2.012	77.32
3	4.866	3.703	2.522
3	4.274	1.562	33.82
3	4.054	1.589	42.99
3	3.862	1.619	96.05
3	4.1135	1.582	59.02
3	4.3085	1.553	17.17
3	4.623	1.510	8.060
3	3.945	1.203	71.59
3	4.161	1.375	23.54
3	4.357	1.424	15.48
4	4.407	5.881	20.27[a]
4	4.023	6.005	46.61[a]
4	3.724	1.021	182.9
4	4.144	0.9954	30.90
4	3.702	1.031	129.3
4	3.820	2.665	140.6
4	4.168	1.970	32.52
4	4.902	1.843	5.187
4	3.975	2.004	70.00
4	3.867	2.024	86.48
4	4.218	2.941	34.00
4	3.879	3.035	76.85
4	4.279	2.938	25.08
4	4.796	3.717	4.116
4	4.554	3.802	8.272
4	4.378	3.859	17.92
4	4.241	3.904	27.06
4	4.914	3.667	2.798
5	4.232	2.005	28.50
5	3.975	2.051	71.87
5	3.867	1.663	105.2
5	4.196	4.029	30.20
5	4.523	3.909	12.14
5	4.472	1.963	10.34
5	4.625	1.932	8.944
5	4.146	2.013	38.62
5	3.757	2.081	122.0
5	4.207	2.001	38.34
5	4.407	1.966	24.33
5	4.407	2.963	15.75
5	4.421	2.958	17.65
5	4.170	3.024	39.40
5	4.382	3.954	17.70
5	3.855	2.700	109.2

$k_{obs\text{-}H_2}=\frac{-1}{[COF_2]_0[M]}\left.\frac{d[COF_2]}{dt}\right|_0$ (values in table computed from COF_2 emission data)

[M] = total concentration

Units of cubic centimeters, mole, °K, sec

[a] Corrected for optical depth.

$$\left.\frac{d[COF_2]}{dt}\right|_0 = -k_{obs\text{-}H_2}[COF_2]_0[M] , \qquad (4)$$

where $[COF_2]_0$ is the initial concentration of COF_2, and [M] is the total concentration. Variation of the initial concentration of hydrogen by a factor of approximately 4, initial hydrogen percentages from 1%–4%, did not significantly influence the initial rate of reaction of COF_2, as indicated in Eq. (4), where $b\sim 0$. Hence, the empirical rate equation, Eq. (4), does not include an explicit dependency on the initial concentration of hydrogen. In this study, Eq. (4) was used to determine $k_{obs\text{-}H_2}$ for each data point.

The numerical values of $k_{obs\text{-}H_2}$ for the COF_2–H_2 reaction system computed from COF_2 emission data are listed in Table V, and an Arrhenius plot for $k_{obs\text{-}H_2}$ is presented in Fig. 5. A least mean squares fit of the COF_2 emission data resulted in

$$k_{obs\text{-}H_2} = 10^{14.61\pm 0.14} \times \exp(-66\,900 \pm 1600/RT)\ \text{cc/mole}\cdot\text{sec} . \qquad (5)$$

Also shown in Fig. 5 are the computed results for $k_{obs\text{-}H_2}$ obtained from the HF emission data. These results are based on the steady-state solution, $\frac{1}{2}d[HF]/dt = -d[COF_2]/dt$, of the six step reaction mechanism which was developed in the study (see COF_2–H_2 Mechanism and Discussion). The numerical values of the observed rate constants for the COF_2–H_2 system computed from HF emission data, based on this steady-state solution, are listed in Table VI using the notation $k^{(HF)}_{obs\text{-}H_2}$.

IV. THE COF_2–H_2 MECHANISM

In order to gain more insight into the COF_2–H_2 reaction system, an analytical study was initiated with the goal of developing a plausible mechanism for the reac-

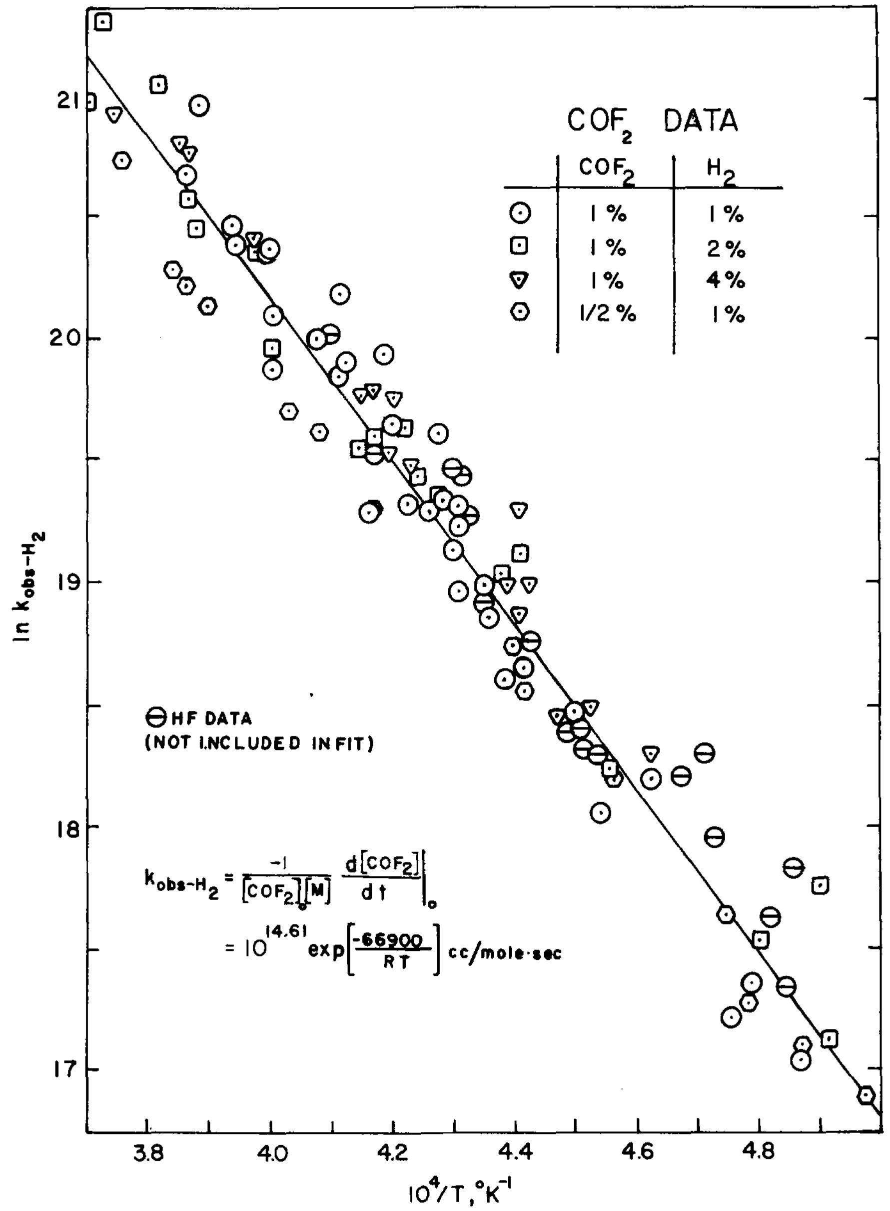

FIG. 5. Arrhenius plot of the observed rate constant for the reaction of COF_2 in the presence of H_2.

tion system. Twenty-two potential elementary reaction steps out of more than the 100 reactions considered are listed in Table VII. These reactions were screened to determine the potentially important steps of the mechanism. An equivalent reaction mechanism was employed to study the effects of CO_2, H_2O, and O_2 impurities, and these type reactions were shown to have an insignificant effect on the COF_2–H_2 data. In these studies, median literature values of the rate constants were used whenever possible and the rate constants for all other reactions were estimated using thermochemical and other appropriate estimating techniques.[7–9]

The rates of all reactions considered were evaluated under characteristic experimental conditions, and the following six reactions were found to dominate the COF_2–H_2 reaction system:

$$COF_2 + M \xrightarrow{1} COF + F + M \ ,$$

$$COF + M \xrightarrow{2} CO + F + M \ ,$$

$$H_2 + M \xrightarrow{10} H + H + M \ ,$$

$$F + H_2 \xrightarrow{12} HF + H \ ,$$

$$H + COF_2 \xrightarrow{18} COF + HF \ ,$$

$$H + COF \xrightarrow{20} CO + HF \ .$$

The initial computations also indicated that, in general, the rate of Reaction (10) was small compared to the rates of the other reactions. This result was later used in the steady-state analysis of the proposed mechanism. The initially estimated rate constant values for these six reactions which were used to examine analytically the potential reaction mechanism in Table VII were obtained as follows. The rate constant for Reaction (1), as discussed previously, was based on Eq. (1) from the pure COF_2 decomposition study. The rate constants for Reactions (10) and (12) were obtained from median values reported in the literature. The activation energy for Reaction (2) was initially assigned the low pressure RRK theory prediction of 53.1 kcal/mole based on the mid-range temperature of 2300 °K, the JANAF[4] heats of formation at 0 °K of F and CO, and the experimental heat

TABLE VI. Comparison of the initial reaction rates of COF_2 and HF in the high temperature COF_2–H_2 system.

$10^4/T$	$[M]\times 10^5$	$R_{HF}\times 10^3$	R_{COF_2}/R_{HF}	$k^{(HF)}_{obs\text{-}H_2}\times 10^{-7}$
4.419	3.8	3.918	0.519	13.57
4.854	3.65	0.913	0.475	3.43
4.521	3.76	2.482	0.569	8.78
4.728	3.71	1.707	0.401	6.20
4.715	3.71	2.404	0.297	8.73
4.367	3.83	4.79	0.514	16.33
4.308	3.84	8.39	0.359	28.45
4.675	1.86	0.544	0.378	7.86
4.866	1.83	0.373	0.281	5.57
4.824	1.84	0.304	0.401	4.49
4.548	1.87	0.607	0.525	8.68
4.320	1.92	1.68	0.431	22.79
4.507	1.89	0.734	0.509	10.27
4.320	1.91	1.97	0.364	27.00
4.188	1.94	2.27	0.508	30.16
4.103	1.96	4.28	0.366	55.71
4.533	1.88	0.659	0.514	9.32

$[M]\approx$ total concentration, $[COF_2]_0=0.01\ [M]$

Units of cubic centimeters, °K, mole, sec

$R_{COF_2}\equiv -\left.\frac{d[COF_2]}{dt}\right|_0 \approx 10^{14.61}\exp(-66\,900/RT)[COF_2]_0[M]$ (this study computed from COF_2 emission data)

$R_{HF}=\left.\frac{d[HF]}{dt}\right|_0$ (from HF emission data)

$k^{(HF)}_{obs\text{-}H_2}=\frac{1}{2}\left.\frac{d[HF]}{dt}\right|_0 \frac{1}{[COF_2]_0[M]}$ (values in table computed from HF emission data based on steady state solution $\frac{1}{2}\,d[HF]/dt = -d[COF_2]/dt$)

of formation of COF at 0 °K, $\Delta H^\circ_{f0}(COF)$, from the COF_2 study (see Discussion). The preexponential factor of Reaction (2) was initially estimated to be 10^{14}–10^{16}, in line with analogous unimolecular reactions. Semenoff's rule[7] was used to estimate the activation energies of Reactions (18) and (20), E_{18} and E_{20}, based on the experimental value of $\Delta H^\circ_{f0}(COF)$ from the COF_2 study and literature[1,4] values of $\Delta H^\circ_{f0}(COF)$. For these reactions, $E_{20}\sim 0$ kcal/mole and $E_{18}\sim 0$–10 kcal/mole with the midrange value of $E_{18}\sim 5$ kcal/mole. The preexponential factors for Reactions (18) and (20) were estimated using collision numbers and steric factors obtained from analogous H atom abstraction reactions.

V. DISCUSSION

A. Kinetics

A steady-state analysis in H, F, and COF for the proposed six step COF_2–H_2 mechanism, assuming that the rate of Reaction (10) is small compared to the other reaction rates, yields

$$-\frac{d[COF_2]}{dt}=\left(k_1+\left[\frac{k_1k_2k_{18}}{k_{20}}\right]^{1/2}\right)[COF_2][M] \qquad (6)$$

and

$$-\frac{d[COF_2]}{dt}=\frac{1}{2}\,\frac{d[HF]}{dt}\ . \qquad (7)$$

Experimentally, the over-all rate of COF_2 disappearance was found to be independent of the H_2 concentration and follow the expression

$$-\frac{d[COF_2]}{dt}=k_{obs\text{-}H_2}[COF_2][M]\ .$$

The steady state expression given by Eq. (6) is also independent of the H_2 concentration and is of the same form as the experimental result where

$$k_{obs\text{-}H_2}=k_1+\left[\frac{k_1k_2k_{18}}{k_{20}}\right]^{1/2}\ .$$

Also in agreement with the steady-state analysis in Eq. (7) is the fact that experimentally the initial rate of COF_2 disappearance was found to be approximately one-half the initial rate of HF formation at the same temperature and pressure as shown in Table VI. In addition, when the steady-state solution given by Eq. (7) is used with the experimental rate data for HF, the computed $k_{obs\text{-}H_2}$ for HF given in Table VI, $k^{(HF)}_{obs\text{-}H_2}$, is essentially equal to the $k_{obs\text{-}H_2}$ computed from COF_2 rate data as shown in the Arrhenius plot in Fig. 5.

The given equations may be combined as

$$k_{(obs\text{-}H_2)_{corr}}=(k_{obs\text{-}H_2}-k_1)=\frac{-d[COF_2]}{dt}\,\frac{1}{[COF_2][M]}-k_1$$
$$=\left[\frac{k_1k_2k_{18}}{k_{20}}\right]^{1/2}\ . \qquad (8)$$

The left hand side of Eq. (8) is the observed rate of COF_2 reaction in the presence of H_2 corrected for the minor contribution of COF_2 decomposition via $COF_2+M\xrightarrow{k_1}COF+F+M$. When the contribution of Reaction (1) to the over-all rate of COF_2 decomposition is accounted for by using the value of k_1 given by Eq. (1) with the $k_{obs\text{-}H_2}$ data in Table V, the resulting Arrhenius expression is

$$k_{(obs\text{-}H_2)_{corr}}=10^{14.48\pm0.15}$$
$$\times\exp[-65\,600\pm1600/RT]\ \text{cc/mole}\cdot\text{sec}\ .$$

This expression for $k_{(obs\text{-}H_2)_{corr}}$ when used in Eq. (8) gives

TABLE VII. Potential reactions in the high temperature COF_2–H_2 reaction system.

	Reference	Comments on method of rate constant evaluation
1. $COF_2+M\rightarrow COF+F+M$	1,2	See text
2. $COF+M\rightarrow CO+F+M$		See text
3. $COF_2+F\rightarrow COF+F_2$	1	Estimated
4. $COF+F_2\rightarrow COF_2+F$	1	Estimated
5. $COF+F\rightarrow CO+F_2$	1	Estimated
6. $COF+COF\rightarrow COF_2+CO$	1	See text
7. $COF_2+CO\rightarrow COF+COF$	1	See text
8. $F_2+M\rightarrow F+F+M$	a	
9. $F+F+M\rightarrow F_2+M$		Reverse fit
10. $H_2+M\rightarrow H+H+M$	13,14,15	
11. $H+H+M\rightarrow H_2+M$		Reverse fit
12. $F+H_2\rightarrow HF+H$	10,11,12	
13. $H+HF\rightarrow H_2+F$	b, c	
14. $HF+M\rightarrow H+F+M$	b, c	
15. $H+F+M\rightarrow HF+M$		Reverse fit
16. $H+F_2\rightarrow HF+F$		Estimated
17. $HF+F\rightarrow H+F_2$		Estimated
18. $H+COF_2\rightarrow COF+HF$		Estimated
19. $COF+HF\rightarrow COF_2+H$		Estimated
20. $H+COF\rightarrow CO+HF$		Estimated
21. $CO+HF\rightarrow H+COF$		Estimated
22. $COF+H_2\rightarrow COFH+H$		Estimated

[a] R. W. Diesen, J. Chem. Phys. 44, 3662 (1966).

[b] J. A. Blauer, J. Chem. Phys. 72, 79 (1968).

[c] T. A. Jacobs, R. R. Giedt, and N. Cohen, J. Chem. Phys. 43, 3688 (1966).

TABLE VIII. Proposed mechanism for the high temperature COF_2–H_2 reaction system.

Reaction	Rate constant[a]	Reference
$COF_2 + M \xrightarrow{1} COF + F + M$	$k_1 = 10^{14.25} \exp(-77\,200/RT)$	This study
$COF + M \xrightarrow{2} CO + F + M$	$k_2 = 10^{15.0} \exp(-49\,000/RT)$	This study
$H_2 + M \xrightarrow{10} H + H + M$	$k_{10} = 10^{18.735} T^{-1.0} \exp(-103\,720/RT)$	15
$F + H_2 \xrightarrow{12} HF + H$	$k_{12} = 4.85 \times 10^{13} \exp(-2470/RT)$	12
$H + COF_2 \xrightarrow{18} COF + HF$	$k_{18} = 10^{12} T^{1/2} \exp(-5000/RT)$	Estimated
$H + COF \xrightarrow{20} CO + HF$	$k_{20} = 10^{12.3} T^{1/2}$	Estimated

[a] Rate constant units cc/mole • sec.

$$10^{14.48} \exp[-65\,600/RT] = \left[\frac{k_1 k_2 k_{18}}{k_{20}}\right]^{1/2} . \qquad (9)$$

If Eq. (9) is used with the experimental rate constant for $k_1 = 10^{14.25} \exp(-77\,200/RT)$ cc/mole · sec and the estimated expressions given in Table VIII for $k_{18} = 10^{12} T^{1/2} \times \exp(-5000/RT)$ cc/mole · sec and $k_{20} = 10^{12.3} T^{1/2}$ cc/mole · sec, an experimental rate constant for k_2 is determined to be

$$k_2 = 10^{15.0} \exp[-49\,000/RT] \text{ cc/mole} \cdot \text{sec} .$$

The major sources of uncertainty in this rate constant for k_2 stem from the estimated rate constants for Reactions (18) and (20). The error in the preexponential term of k_2 would be the uncertainty associated with the ratio of the preexponential factors of k_{20} and k_{18} equal to 2 and the error in the activation energy of k_2 would be the uncertainty associated with the difference of the corresponding activation energies, $E_{18} - E_{20}$, equal to 5 kcal/mole.

In order to investigate the proposed mechanism for COF_2–H_2 further and to substantiate analytically the steady state analysis, the proposed mechanism and rate constants in Table VIII were integrated for typical experimental conditions. The instantaneous reaction rates for each reaction of the proposed six step mechanism are shown for a typical case in Fig. 6, and the corresponding species concentrations are shown in Fig. 7. Analysis of these results indicates that the H, F. and COF species concentrations may be considered to be in a steady state and that the rate of Reaction (10) is small compared to the rates of the other reactions. In addition, the computed COF_2 and HF concentration profiles were compared to the experimental concentration profiles. A typical result, at the midrange experimental temperature, of these comparison computations with the rate constants in Table VIII is shown in Fig. 8. In general, the computed and the experimental HF and COF_2 concentration profiles agreed when the median literature values of k_{12} and k_{10} given in Table VIII were used in the numerical integration scheme. In addition, since k_{12} and k_{10} were not used directly in the analytical steady-state solution for the experimental value of k_2, a sensitivity analysis of the effects on the proposed mechanism in Table VIII of higher and lower literature values of k_{12} and k_{10} was performed. These computations indicated that the computed and the experimental HF and COF_2 concentration profiles agreed even when different literature[10–12] values of k_{12} were used with the other rate constants in Table VIII. For the experimental conditions given in Fig. 8, a value of $k_{12} = 1.6 \times 10^{14} \exp(-1600/RT)$ cc/mole · sec[10] produced comparison results which were almost exactly the same as those shown in Fig. 8. Similar computations with different literature[13–15] values of k_{10} also showed good agreement in computed and experimental profiles. A $k_{10} = 10^{14} \exp(-97\,200/RT)$ cc/mole · sec[13] produced comparison results which were effectively the same as those shown in Fig. 8 and a $k_{10} = 10^{21} T^{-1.5} \exp(-103\,200/RT)$ cc/mole · sec[14] produced results which were even better than those shown in Fig. 8. Also, since k_2 was determined in the steady state solution as the ratio of four other experimental and estimated rate constants, i.e., $k_{(\text{obs}-H_2)_{\text{corr}}}$, k_1, k_{18}, k_{20}, additional sensitivity analysis of the proposed mechanism and rate constants in Table VIII was conducted. These computations indicated that a slight change in the preexponential factor of k_2 would allow the experimental and computed COF_2 and HF profiles to agree almost exactly as shown in Fig. 8. These comparison results demonstrate the consistency of the rate constants and reaction steps used in the proposed six step mechanism for the COF_2–H_2 system.

Additional computer integration for the COF_2 decomposition mechanism shown in Fig. 9 with the rate constants for Reactions (1) and (2) obtained in this study given in Table VIII also shows good agreement between experimental and predicted COF_2 species concentrations as shown in Fig. 9. For these computations, the activation energies of the rate constants of Reactions (3), (4), and (5) were estimated to be $E_3 \sim 65$ kcal/mole, $E_4 \sim 0$ kcal/mole, and $E_5 \sim 25$ kcal/mole based on the experimental $\Delta H^\circ_{f0}(COF) = -66$ kcal/mole (see Sec. V. B). The preexponential factors of Reactions (3), (4), and (5) were used as given in Table I, and the rate constants

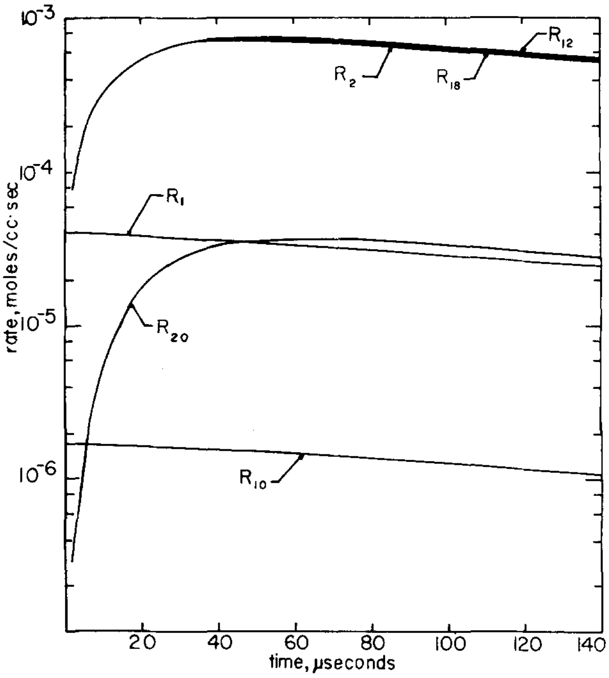

FIG. 6. Computed rates: $T = 2334$ °K; $[M] = 0.1938 \times 10^{-4}$ moles/cc; 1% COF_2–1% H_2.

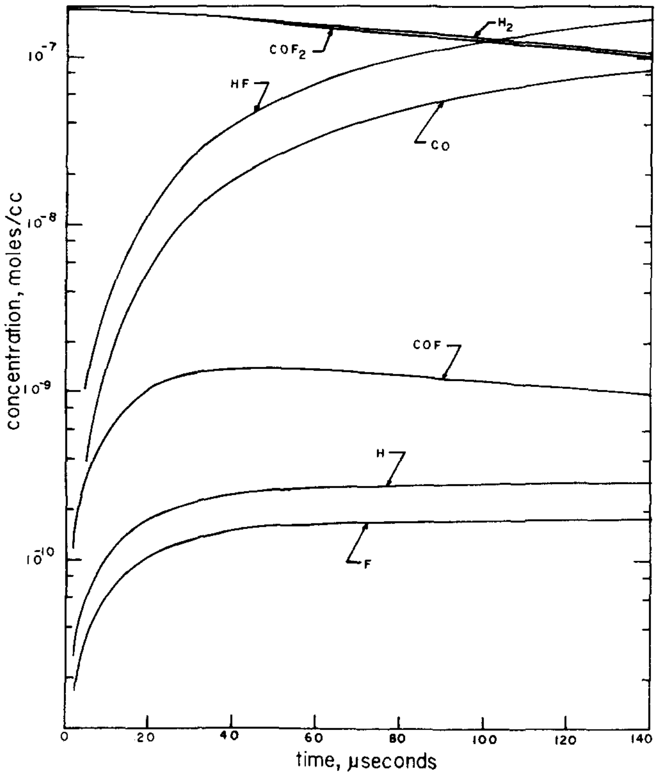

FIG. 7. Computed species profiles: $T = 2334\,°K$; $[M] = 0.1938 \times 10^{-4}$ moles/cc; 1% COF_2–1% H_2.

of Reactions (8) and (9) are also listed in Table I.

Both the experimental results and the numerically integrated profiles for COF_2 obtained during the course of this study indicate that the previously estimated value of $k_7 = 10^{11}T^{1/2}\exp(-11\,656/T)$ cc/mole · sec, [1] which was based on the assumed[1] $\Delta H^\circ_{f0}(COF) = -77.4$ kcal/mole, is too high. The experimental data for the CO–COF_2 system given in Table IV indicate that this k_7 is too high by at least a factor of 15. The heat of formation of COF obtained in this study, $\Delta H^\circ_{f0}(COF) = -66$ kcal/mole (see Sec. V. B), may be used with JANAF[4] data for COF_2 and CO to estimate the activation energy of Reaction (7) as $E_7^* \sim 45$ kcal/mole. When this activation energy is combined with the previously estimated[1] preexponential factor for Reaction (7), an estimate for k_7 consistent with the results of this study is given by $k_7^* = 10^{11}T^{1/2}\exp \times (-45\,000/RT)$ cc/mole · sec. Comparison of k_7^* and the k_7 from Ref. 1 at the COF_2 study midrange temperature of 2900 °K indicates that the previously estimated[1] k_7 is higher by a factor of 44 than justified by this study's $\Delta H^\circ_{f0}(COF)$. In addition, the numerically integrated profiles of COF_2 for either the COF_2–H_2 reaction system or the COF_2 decomposition system were shown to be basically unchanged with the inclusion of Reactions (6) and (7) in the appropriate mechanisms when the numerical value of k_7 was set equal to k_7^*.

B. Thermochemistry

The results of the COF_2–H_2 study may be used to estimate the dissociation energy at 0 °K of the F–CO bond, $D_0^\circ(F{-}CO)$, by employing the RRK theory for low pressure reactions where $D_0^\circ(F{-}CO) = E_2 + (s - 3/2)RT$. The number of effective oscillators, s, may be calculated using the technique suggested by Refs. 8 and 16, where $s \equiv C_{vib}/R = (C_p - 4R)/R$ with C_p for COF obtained from tabulated heat capacity tables such as JANAF.[4] An estimated $s \sim C_{vib}/R \sim 2.85$ may be employed with the COF_2–H_2 study experimental midrange temperature of 2300 °K and $E_2 = 49.0$ kcal/mole to predict that $D_0^\circ(F{-}CO)$ equals 55.2 kcal/mole. This experimental value of $D_0^\circ(F{-}CO)$ leads to an experimental estimated value of the heat of formation at 0 °K of COF, $\Delta H^\circ_{f0}(COF)$, given as $\Delta H^\circ_{f0}(COF) = -64.0$ kcal/mole when the JANAF[4] heats of formation at 0 °K of F, $\Delta H^\circ_{f0}(F) = 18.36 \pm 0.4$ kcal/mole, and CO, $\Delta H^\circ_{f0}(CO) = -27.2 \pm 0.04$ kcal/mole, are used with $COF \rightarrow CO + F + 55.2$ kcal and $55.2 = \Delta H^\circ_{f0}(F) + \Delta H^\circ_{f0}(CO) - \Delta H^\circ_{f0}(COF)$.

The heat of formation of COF at 0 °K can also be determined from the results of the COF_2 study where $D_0^\circ(F{-}COF) = E_1 + (s - 3/2)RT$. The resulting dissociation energy, obtained by employing an estimated $s \sim C_{vib}/R \sim 5.85$ for COF_2 with the COF_2 study experimental midrange temperature of 2900 °K and $E_1 = 77.2$ kcal/mole, is $D_0^\circ(F{-}COF) = 102.3$ kcal/mole. This experimental value of $D_0^\circ(F{-}COF)$ leads to an experimental estimated

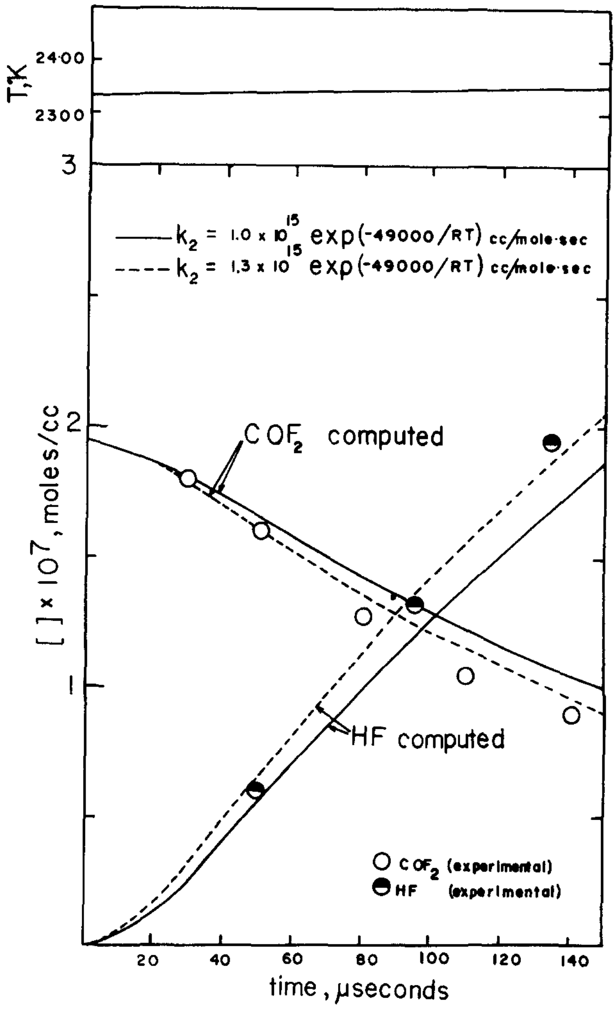

FIG. 8. Comparison of predicted and experimental profiles for COF_2 and HF: $T = 2334\,°K$; $[M] = 0.1938 \times 10^{-4}$ moles/cc; 1% COF_2–1% H_2.

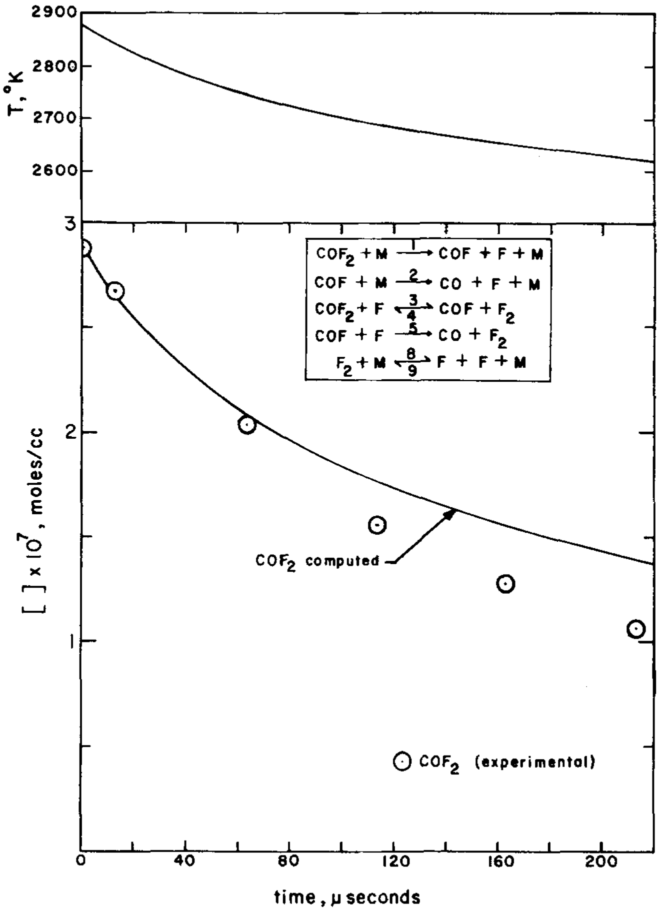

FIG. 9. Comparison of predicted and experimental profiles for the thermal decomposition of COF_2: $T = 2877\,°K$; $[M] = 0.29 \times 10^{-4}$ moles/cc; 1% COF_2.

value of $\Delta H^\circ_{f0}(COF) = -68.1$ kcal/mole when the JANAF[4] heats of formation at 0 °K of F and COF_2, $\Delta H^\circ_{f0}(COF_2) = -152.0 \pm 0.4$ kcal/mole, are used with $COF_2 \rightarrow COF + F + 102.3$ kcal and $102.3 = \Delta H^\circ_{f0}(F) + \Delta H^\circ_{f0}(COF) - \Delta H^\circ_{f0}(COF_2)$. This compares favorably with the experimental value of $\Delta H^\circ_{f0}(COF) = -64.0$ kcal/mole which was obtained in the COF_2–H_2 study. Thus, $\Delta H^\circ_{f0}(COF)$ must be approximately the average value of -66 kcal/mole.

If the experimental value of $D^\circ_0(F-COF) = 102.3$ kcal/mole from the COF_2 decomposition study is used in conjunction with the experimental value of $D^\circ_0(F-CO) = 55.2$ kcal/mole from the COF_2–H_2 study, it is possible to calculate via

$$COF_2 \rightarrow COF + F + 102.3 \text{ kcal} \qquad (10)$$

$$+ COF \rightarrow CO + F + 55.2 \text{ kcal} \qquad (11)$$

that experimentally

$$COF_2 \rightarrow CO + 2F + 157.5 \text{ kcal} . \qquad (12)$$

Since the experimental dissociation energies in Eqs. (10) and (11) were computed only with the use of the low pressure RRK prediction for $D^\circ_0(F-COF)$ and $D^\circ_0(F-CO)$ which were obtained from experimental and estimated activation energies with estimates of $s \sim C_{vib}/R$, JANAF[4] table data for Eq. (12) may be used for comparison. When the JANAF[4] table is used to evaluate the heat of reaction at 0 °K for $COF_2 \rightarrow CO + 2F$, a value of 161.5 ± 1.2 kcal is obtained, which agrees closely with the experimental value of 157.5 kcal. Using this result and considering that the experimental heat of reaction in Eq. (12) is the sum of the two experimental dissociation energies given in Eqs. (10) and (11) from two different studies, verification of the consistency of the studies and of the experimental values of the dissociation energies is obtained. These experimental dissociation energies were used to compute this study's average experimental value of $\Delta H^\circ_{f0}(COF) = -66$ kcal/mole which leads to average experimental values of $D^\circ_0(F-COF) = 104.3$ kcal/mole and $D^\circ_0(F-CO) = 57.2$ kcal/mole when JANAF[4] heats of formation at 0 °K of COF_2, F, and CO are used in the calculations.

The average experimental values of $D^\circ_0(F-COF) = 104.3$ kcal/mole, $D^\circ_0(F-CO) = 57.2$ kcal/mole, and $\Delta H^\circ_{f0}(COF) = -66$ kcal/mole may be compared to the values available in the literature. Owing to a lack of experimental data, the JANAF[4] tables estimated $\Delta H^\circ_{f0}(COF)$ by equating the ratio of the first and second C–F bond dissociation energies of COF_2 to the ratio of the first and second C–Cl bond dissociation energies of $COCl_2$:

$$\frac{D^\circ_0(F-COF)}{D^\circ_0(F-CO)} = \frac{D^\circ_0(Cl-COCl)}{D^\circ_0(Cl-CO)} = 4$$

With this ratio and the sum of the C–F bond dissociation energies of COF_2 obtained from $COF_2 \rightarrow CO + 2F + 161.5$ kcal,[4] estimated values of $D^\circ_0(F-COF)$ and $D^\circ_0(F-CO)$ may be calculated. The reaction $COF_2 \rightarrow F + COF + D^\circ_0(F-COF)$ may then be used with JANAF[4] data for F and COF_2 to estimate $\Delta H^\circ_{f0}(COF)$. Based on the considerable uncertainty of this estimating technique, the JANAF[4] tables report a value of $\Delta H^\circ_{f0}(COF) = -41 \pm 15$ kcal/mole. With the JANAF[4] data, the first and second C–F bond dissociation energies of COF_2 are $D^\circ_0(F-COF) = 129.4 \pm 16$ kcal/mole and $D^\circ_0(F-CO) = 32.1 \pm 15$ kcal/mole. This general type of estimating procedure was followed in Ref. 1 using what was considered to be a more reasonable analogy consistent with fluorcarbon chemistry. The analogy used by Ref. 1 was based on equating the ratio of the first and second C–F bond dissociation energies of COF_2 to the first and second bond dissociation energies of CF_4:

$$\frac{D^\circ_0(F-COF)}{D^\circ_0(F-CO)} = \frac{D^\circ_0(F-CF_3)}{D^\circ_0(F-CF_2)} = 1.34 .$$

Based on this analgoy, Modica[1] computed estimated values of $D^\circ_0(F-COF) = 91.9$ kcal/mole, $D^\circ_0(F-CO) = 68.6$ kcal/mole, and $\Delta H^\circ_{f0}(COF) = -77.4$ kcal/mole. Henrici, Lin, and Bauer[17] studied the reaction of F_2O with CO and found that the heating effect of this reaction, based on a postulated mechanism, was strongly dependent on the concentration of the COF radical. They estimated the enthalpy of formation of COF to be -34 ± 5 kcal/mole at 25 °C. When JANAF[4] data are also used, this value results in $D^\circ_0(F-COF) = 136.4$ kcal/mole, $D^\circ_0(F-CO) = 25.1$ kcal/mole, and

$$\frac{D^\circ_0(F-COF)}{D^\circ_0(F-CO)} = 5.43 .$$

For comparison with these references, the average experimental dissociation energies obtained in this study result in

$$\frac{D_0^\circ(\mathrm{F-COF})}{D_0^\circ(\mathrm{F-CO})} = 1.82 \ .$$

This ratio of the bond dissociation energies D_0°(F–COF)/D_0°(F–CO) as experimentally determined in this study lies between the previously estimated values which were employed by JANAF[4] and Modica[1] to estimate ΔH°_{f0}(COF). Since the present result for ΔH°_{f0}(COF) is based on experimental data rather than estimating procedures and falls between the previously estimated values, it is suggested that the best available value for ΔH°_{f0}(COF) is −66 kcal/mole.

ACKNOWLEDGMENT

This study was supported by the Air Force Office of Scientific Research under Grant Number AF-AFOSR-71-2125A. The authors would also like to acknowledge the assistance of Mr. M. Fling and Mr. S. Lesko in the acquisition of the experimental data.

---

*Present address: KVB Engineering, 17332 Irvine Blvd., Tustin, CA 92680.

†Present address: Assistant Professor, University of British Columbia, Vancouver, British Columbia, Canada.

[1] A. P. Modica, J. Phys. Chem. **74**, 1194 (1970).

[2] D. M. Weston and R. A. Matula, Combust. Sci. Tech. **4**, 37 (1971).

[3] D. M. Weston, Ph.D. thesis, Drexel University, Philadelphia, PA, 1970.

[4] Natl. Bur. Stand. Ref. Data Ser. **37** (1971).

[5] T. N. Adams, D. M. Weston, and R. A. Matula, J. Chem. Phys. **55**, 5674 (1971).

[6] R. F. Sawyer, and P. Purgalis, "General Formulation and Numerical Solution of Reaction Rate Problems," Report No. TS-68-4, University of California, Berkeley, June, 1968.

[7] K. J. Laidler, *Chemical Kinetics* (McGraw-Hill, New York, 1965).

[8] S. W. Benson, *Thermochemical Kinetics* (Wiley, New York, 1968).

[9] A. A. Frost and R. G. Pearson, *Kinetics and Mechanisms* (Wiley, New York, 1961).

[10] H. G. Wagner, and J. Wolfrum, Angew. Chem. **83**, 561 (1971) [reference in K. L. Kompa and J. Wanner, Chem. Phys. Lett. **12**, 560 (1972).]

[11] D. A. Bittker, Natl. Aeron. Space Admin. Tech. Note D-3607, August, 1966.

[12] R. Foon, and G. P. Reid, Trans. Faraday Soc. **67**, 3513 (1971).

[13] W. S. Watt, and A. A. Myerson, 6th Int. Shock Tube Symp., Freiburg, 1967, Phys. Fluids. [reference in J. Von Troe, and H. Gg. Wagner, Ber. Bunsenges. 937 (1967)].

[14] W. G. Burnell, V. S. Sarli, and T. F. Zupnik, United Aircraft Corp. Paper for Third Conference on Performance of High Temperature Systems, 04410, December, 1964) [reference in Pyrodynamics **4**, 371 (1966).]

[15] J. P. Rink, J. Chem. Phys. **34**, 262 (1962).

[16] D. M. Golden, R. K. Solly, and S. W. Benson, J. Phys. Chem. **75**, 1333 (1971).

[17] H. Henrici, M. C. Lin, and S. H. Bauer, J. Chem. Phys. **52**, 5834 (1970).